Electronic Supplementary Material (ESI) for Physical Chemistry Chemical Physics.


# *Supporting Information*

Thomas Dresselhaus[a,b], Steffen Easterwiemann[a], David R. Matuschek[a], Constantin G. Daniliuc[a], Oliver Janka[c], Rainer Pöttgen[c], Armido Studer[a], and Johannes Neugebauer[a,b,*]

[a] Organisch-Chemisches Institut, Westfälische Wilhelms-Universität Münster, Corrensstraße 40, 48149 Münster, Germany

[b] Center for Multiscale Theory and Computation, Westfälische Wilhelms-Universität Münster, Corrensstraße 40, 48149 Münster, Germany

[c] Institut für Anorganische und Analytische Chemie, Westfälische Wilhelms-Universität Münster, Corrensstraße 28/30, 48149 Münster, Germany

* Corresponding author: j.neugebauer@uni-muenster.de

**Table of Contents**

## General Information

**Mass spectra** (HRMS–ESI) were recorded on a *Finnigan* MAT 4200S, *Bruker* Daltonics Micro-TOF or a *Micromass* Quatro LCZ (ESI) and peaks are given in *m/z*. **IR spectra** were recorded on a *Digilab* Varian 3100 FT-IR Excalibur Series equipped with a MKII Golden Gate Single Reflection ATR unit. Recorded IR signals are reported in wavelengths ($cm^{-1}$) with the following abbreviation for the intensity of absorption: *s* = strong, *m* = medium, *w* = weak. **Melting points** (M.p.) were measured on a *Stuart* SMP3 melting point apparatus and are uncorrected. **Thin layer chromatography** (TLC) was carried out on *Merck* silica gel 60 F254 plates; detection by UV (irradiation at 254 nm) or dipping into a solution of $KMnO_4$ (1.5 g), $NaHCO_3$ (5.0 g) in $H_2O$ (400 mL), followed by heating. **Flash chromatography** (FC) was performed on silica gel (*Merck*-Si 60: 40 – 63 µm) with a pressure of 0.1 to 0.5 bar. Used eluents are given in parentheses. **Solvents** for FC were distilled before use. **Techniques:** All reactions were performed under air conditions. Solvents were removed under reduced pressure at 40 °C. Purified compounds were further dried under high vacuum. All **reagents** were purchased of the following companies and have been used without further purification: *Sigma-Aldrich*, *Alfa Aesar*.

## Experimental Procedures

The precursor compound, 2,4-diphenylcarbonohydrazide, was synthesized in accordance to a literature procedure.[1,2] All verdazyl radicals were synthesized in accordance to literature procedures[2] (see scheme S1).

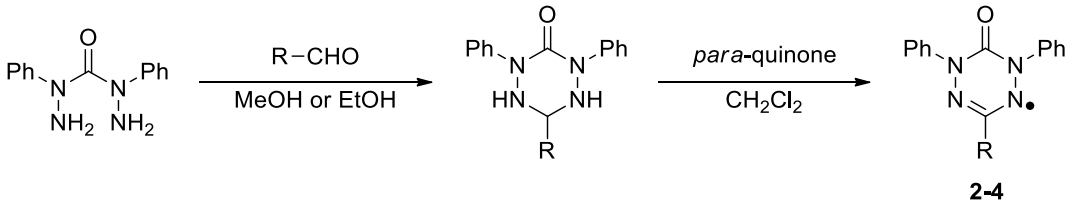


**Scheme S1** General reaction sequence for the preparation of verdazyl radicals.

**1,5-Diphenyl-3-anthracenyl-6-oxo-verdazyl radical** (**2**) was synthesized in accordance to a literature procedure.[2]

**1,5-Diphenyl-3-(4-(diphenylamino)phenyl)-6-oxo-verdazyl radical (3)**

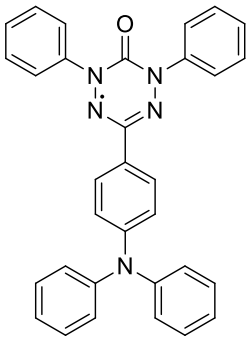

$C_{32}H_{24}N_5O^{\bullet}$
494.57 g/mol

In a two-necked flask with condenser a solution of 4-(diphenylamino)-benzaldehyde (0.47 mL, 1.74 mmol, 1.0 eq.) in EtOH (20 mL) was added to a solution of 2,4-diphenylcarbonohydrazide (420 mg, 1.74 mmol, 1.0 eq.) in EtOH (100 mL) at 80 °C within 15 min and stirring was continued at that temperature for 4 h. Afterwards *para*-quinone (530 mg, 4.94 mmol, 2.7 eq.) was added in one portion and the reaction mixture was stirred at 80 °C for 3 h. The reaction mixture was allowed to cool to rt and the solvent was removed *in vacuo*. FC (*n*-pentane/$CH_2Cl_2$ 5:1) afforded the title compound (0.28 g, 0.57 mmol, 33 %) as a green solid. Single Crystals suitable for X-Ray crystallography were obtained by slow evaporation of a solution of the sample in acetone. **M.p.**: 172 °C; **IR** (ATR, neat): 3062*w*, 1736*w*, 1696*s*, 1588*s*, 1515*m*, 1486*s*, 1458*m*, 1408*m*, 1357*w*, 1315*m*, 1270*s*, 1243*m*, 1173*m*, 1121*m*, 1075*m*, 1027*m*, 915*m*, 894*m*, 835*m*, 750*s*, 734*m*, 714*m*, 690*s*, 656*m*, 634*m*, 616*m*, 600*m*, 548*w*; **HRMS** (ESI): *m/z* = 495.2054, 517.1873 calcd. for $[M+H]^+$, $[M+Na]^+$, found: 495.2050, 517.1876.

**2,4-Diphenyl-6-(4-((trimethylsilyl)ethynyl)phenyl)-1,2,4,5-tetrazinan-3-one (S1)**

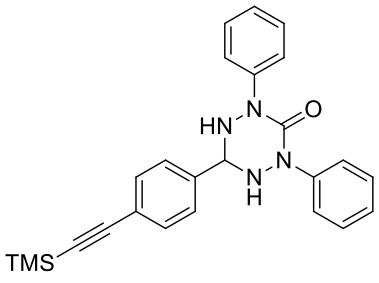

$C_{25}H_{26}N_4OSi$
426.59 g/mol

A solution of 4-((trimethylsilyl)ethynyl)benzaldehyde (303 mg, 1.50 mmol, 1.0 eq.) in MeOH (3 mL) was added within 30 min at 40 °C to a solution of 2,4-diphenylcarbonohydrazide (363 mg, 1.50 mmol, 1.0 eq.) in MeOH (5 mL). The reaction mixture was heated to 60 °C and stirred at that temperature for 3 h. After the mixture was allowed to cool to rt the precipitate was filtered off and washed with little amounts of cold MeOH. The solid was further dried *in vacuo* to afford the title compound (370 mg, 867 µmol, 58 %) as a colorless solid. **M.p.**: 198 °C; **IR** (neat): 3238*w*, 2963*w*, 2158*w*, 1626*m*, 1493*w*, 1361*s*, 1304*s*, 1248*m*, 1222*w*, 1129*w*, 1074*w*, 1052*w*, 915*m*, 846*s*, 756*m*, 692*m*, 643*m*; **$^1$H NMR** (300 MHz, $CDCl_3$): $\delta$ 7.61 – 7.56 (m, 4H, $CH_{arom}$), 7.50 (d, *J* = 8.2 Hz, 2H, $CH_{arom}$), 7.38 (d, *J* = 8.3 Hz, 2H, $CH_{arom}$), 7.31 – 7.19 (m, 4H, $CH_{arom}$), 7.08 – 7.00 (m, 2H, $CH_{arom}$), 5.69 (s, 2H, *N*H), 5.26 (s, 1H, CH), 0.19 (s, 9H, $CH_3$); **$^{13}$C NMR** (75 MHz, $CDCl_3$): $\delta$ 153.7 (C), 142.2 (C), 136.1 (C), 131.4 (CH), 127.7 (CH), 126.4 (CH), 123.8 (C), 122.7 (CH), 121.9 (CH), 104.1 (C), 94.4 (C), 71.3 (CH), -0.5 ($CH_3$); **HRMS** (ESI): *m/z* = 427.1949, 449.1768 calcd. for $[M+H]^+$, $[M+Na]^+$, found: 427.1937, 449.1756.

**1,5-Diphenyl-3-(4-(trimethylsilyl)ethinyl)phenyl-6-oxo-verdazyl (4)**

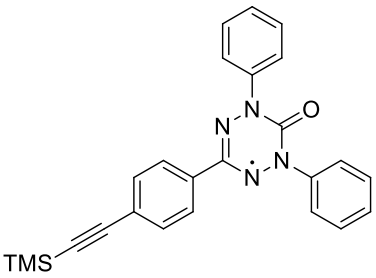


$C_{25}H_{23}N_4OSi^{\bullet}$
423.56 g/mol

In a sealed tube tetrazinan-3-one **S1** (313 mg, 733 µmol, 1.0 eq.) and *para*-quinone (135 mg, 1.25 mmol, 1.7 eq.) were dissolved in $CH_2Cl_2$ (7 mL). The reaction mixture was stirred at 60 °C for 3 h and then allowed to cool to rt. The solvent was removed in vacuo and the residue subjected to FC (*n*-pentane/MTBE, 15:1), which afforded the title compound (288 mg, 680 µmol, 93 %) as a purple solid. Crystals suitable for single crystal X-Ray crystallography were obtained by slow evaporation of a solution of the sample in EtOAc. **M.p.**: 221 °C; **IR** (neat): 2957*w*, 2153*w*, 1700*s*, 1591*w*, 1484*m*, 1408*w*, 1359*w*, 1302*w*, 1244*s*, 1172*w*, 1121*w*, 1025*w*, 841*s*, 745*s*, 683*s*, 635*m*; **HRMS** (ESI): *m/z* = 446.1533, 869.3174 calcd. for $[M+Na]^+$, $[2M+Na]^+$, found: 446.1534, 869.3184.

**1,5-Diphenyl-3-(4-ethinyl)phenyl-6-oxo-verdazyl (5)**

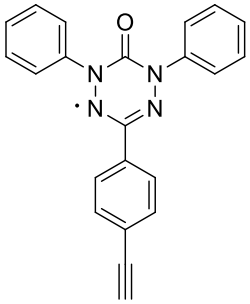

$C_{22}H_{15}N_4O^{\bullet}$
351.38 g/mol

Verdazyl radical **4** (60 mg, 0.14 mmol, 1.0 eq.) was dissolved in MeOH (4 mL). Then KF (11 mg, 0.18 mmol, 1.3 eq.) was added and the reaction mixture was stirred for 2 h at RT. The formed precipitate was filtered off and washed with little amounts of cold MeOH to afford the title compound (40 mg, 0.11 mmol, 81 %) as a dark red solid. **M.p.:** 223 °C (decomp.); **IR** (neat): 3240*m*, 3056*w*, 1695*s*, 1654*m*, 590*m*, 1486*m*, 1413*m*, 1304*m*, 1249*m*, 1175*w*, 1123*m*, 1073*w*, 1020*w*, 884*m*, 844*m*, 765*s*, 689*s*, 648*s*; **HRMS** (ESI): *m/z* = 352.1319, 374.1138 calcd. for $[M+H]^+$, $[M+Na]^+$, found: 352.1311, 374.1136.

## X-Ray Crystal Structures

**X-Ray diffraction:** Data sets were collected with a Nonius Kappa CCD diffractometer. Programs used: data collection, COLLECT (R. W. W. Hooft, Bruker AXS, **2008**, Delft, The Netherlands); data reduction Denzo-SMN (Z. Otwinowski, W. Minor, *Methods Enzymol.* **1997**, *276*, 307-326); absorption correction, Denzo (Z. Otwinowski, D. Borek, W. Majewski, W. Minor, *Acta Crystallogr*. **2003**, *A59*, 228-234); structure solution SHELXS-97 (G. M. Sheldrick, *Acta Crystallogr*. **1990**, *A46*, 467-473); structure refinement SHELXL-97 (G. M. Sheldrick, *Acta Crystallogr*. **2008**, *A64*, 112-122) and graphics, XP (BrukerAXS, **2000**). *R*-values are given for observed reflections, and $wR^2$ values are given for all reflections. Displacement ellipsoids are shown with 30 % probability.

*Exceptions and special features*: For compound **4** the $SiMe_3$ group was found disordered over two positions. Several restraints (SADI, SAME, ISOR and SIMU) were used in order to improve refinement stability.

The X-Ray crystal structures of verdazyl radicals **1**[3] and **2**[2] were reported before.

**X-ray crystal structure analysis of 3:** formula $C_{32}H_{24}N_5O$, $M$ = 494.56, dark red crystal, 0.35 x 0.23 x 0.07 mm, $a$ = 10.1252(3), $b$ = 10.2626(4), $c$ = 13.4382(5) Å, α = 97.847(1), $\beta$ = 97.577(1), γ = 113.879(2)°, $V$ = 1237.6(1) Å$^3$, $\rho_{calc}$ = 1.33 gcm$^{-3}$, μ = 0.1 mm$^{-1}$, empirical absorption correction (0.971 ≤ T ≤ 0.994), $Z$ = 2, triclinic, space group $P\bar{1}$ (No. 2), λ = 0.71073 Å, $T$ = 223(2) K, ω and φ scans, 20889 reflections collected (±$h$, ±$k$, ±$l$), 5035 independent ($R_{int}$ = 0.052) and 4038 observed reflections [$I$>2σ($I$)], 343 refined parameters, $R$ = 0.049, $wR^2$ = 0.127, max. (min.) residual electron density 0.17 (-0.19) e·Å$^{-3}$, hydrogen atoms were calculated and refined as riding atoms.

**X-ray crystal structure analysis of 4:** formula $C_{25}H_{23}N_4OSi$, $M$ = 423.56, red crystal, 0.28 x 0.16 x 0.03 mm, $a$ = 19.1687(2), $b$ = 16.5200(3), $c$ = 17.4270(3) Å, $\beta$ = 123.080(1)°, $V$ = 4624.1(1) Å$^3$, $\rho_{calc}$ = 1.22 gcm$^{-3}$, μ = 0.1 mm$^{-1}$, empirical absorption correction (0.965 ≤ T ≤ 0.996), $Z$ = 8, monoclinic, space group $C2/c$ (No. 15), λ = 0.71073 Å, $T$ = 223(2) K, ω and φ scans, 13781 reflections collected (±$h$, ±$k$, ±$l$), 3940 independent ($R_{int}$ = 0.049) and 2900 observed reflections

[$I$>2σ($I$)], 308 refined parameters, $R$ = 0.063, $wR^2$ = 0.130, max. (min.) residual electron density 0.23 (-0.29) e·Å$^{-3}$, hydrogen atoms calculated and refined as riding atoms.

**X-ray crystal structure analysis of 5:** formula $C_{22}H_{15}N_4O$, $M$ = 351.38, red crystal, 0.12 x 0.03 x 0.02 mm, $a$ = 10.5130(10), $b$ = 18.2406(6), $c$ = 10.6648(6) Å, $\beta$ = 119.261(4)°, $V$ = 1784.2(2) Å$^3$, $\rho_{calc}$ = 1.22 gcm$^{-3}$, μ = 0.1 mm$^{-1}$, empirical absorption correction (0.965 ≤ T ≤ 0.996), $Z$ = 4, monoclinic, space group $P2_1/c$ (No. 14), λ = 1.54178 Å, $T$ = 223(2) K, ω and φ scans, 14936 reflections collected (±$h$, ±$k$, ±$l$), 3096 independent ($R_{int}$ = 0.064) and 2280 observed reflections [$I$>2σ($I$)], 244 refined parameters, $R$ = 0.046, $wR^2$ = 0.127, max. (min.) residual electron density 0.14 (-0.25) e·Å$^{-3}$, hydrogen atoms calculated and refined as riding atoms.

In all of the following figures displacement ellipsoids are shown with 30 % probability.

**1,5-Diphenyl-3-(4-(diphenylamino)phenyl)-6-oxo-verdazyl radical (3)**

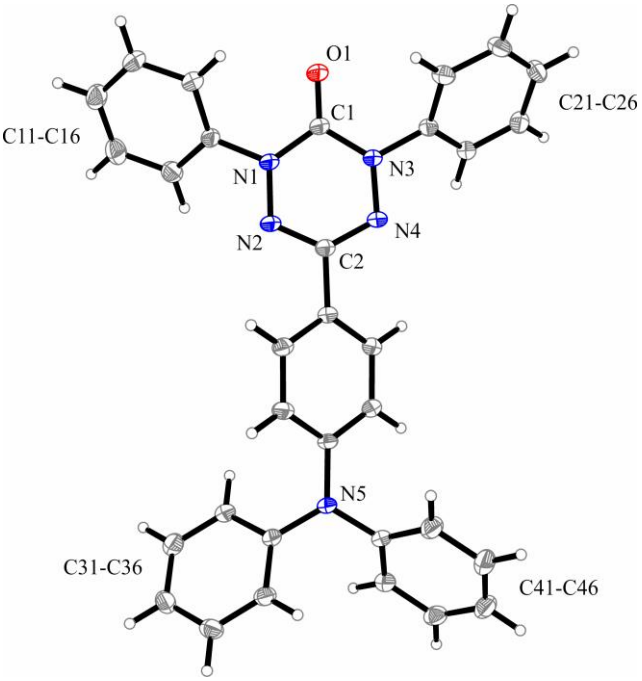


**Figure S1** Molecular structure of compound **3** in the solid state.

**1,5-Diphenyl-3-(4-ethinyl)phenyl-6-oxo-verdazyl (4)**

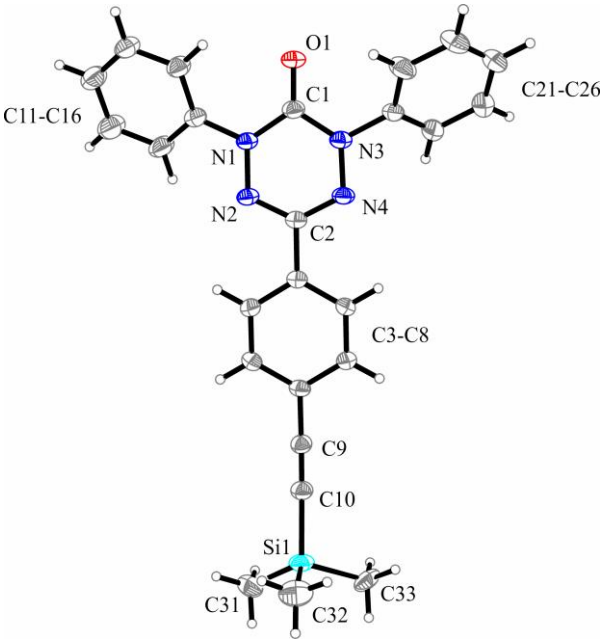


**Figure S2** Molecular structure of compound **4** in the solid state.

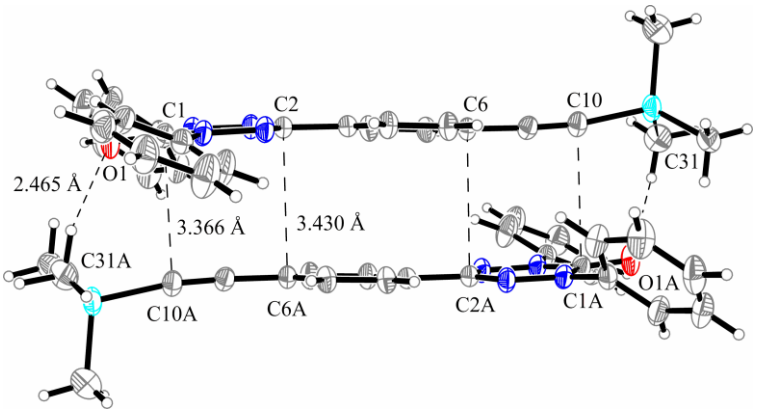


**Figure S3** Representation of the dimer formation through the C-H···O and π ··· π interactions which is responsible for coupling $J_1$ in compound **4.**

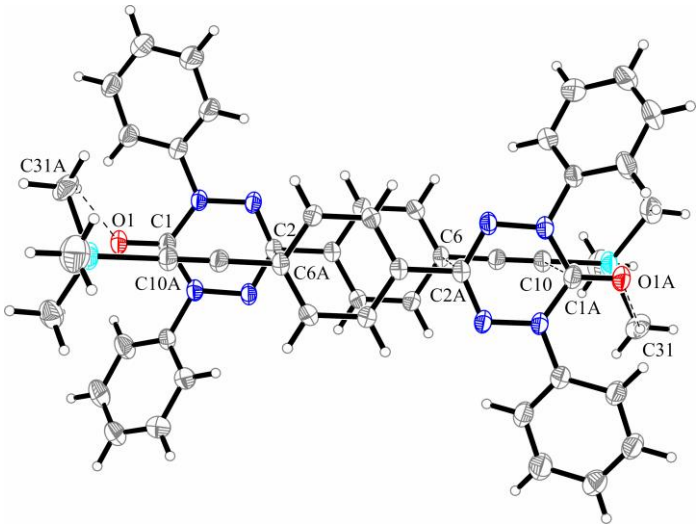


**Figure S4** View perpendicular to the verdazyl radical dimer responsible for coupling $J_1$ in compound **4.**

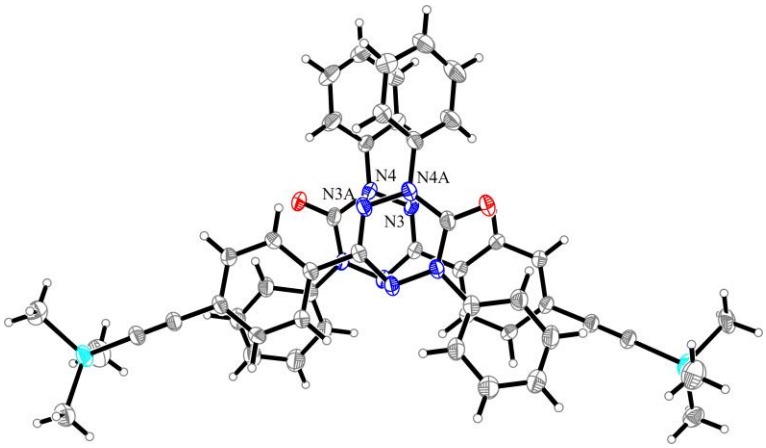


**Figure S5** View perpendicular to the verdazyl radical pair responsible for coupling $J_2$ in compound **4.** The distance between the atoms N3 and N4A (N4 and N3A) is 3.290 Å.

**1,5-Diphenyl-3-(4-ethinyl)phenyl-6-oxo-verdazyl (5)**

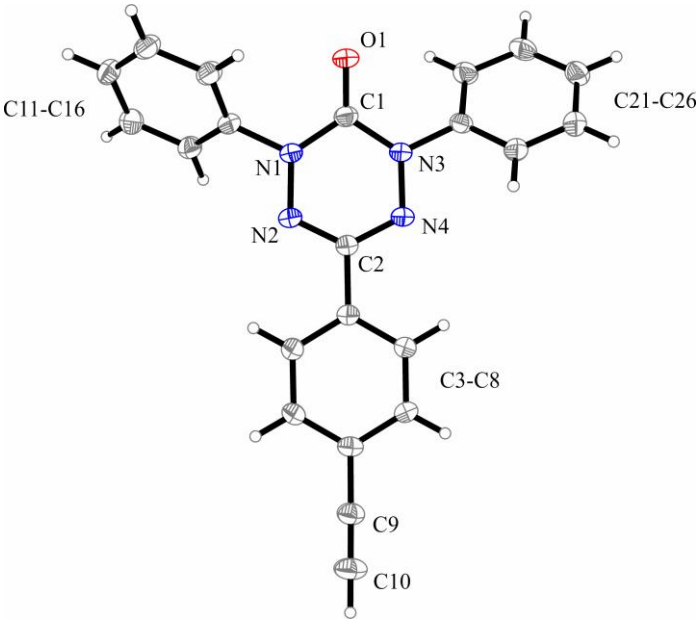


**Figure S6** Molecular structure of compound **5** in the solid state.

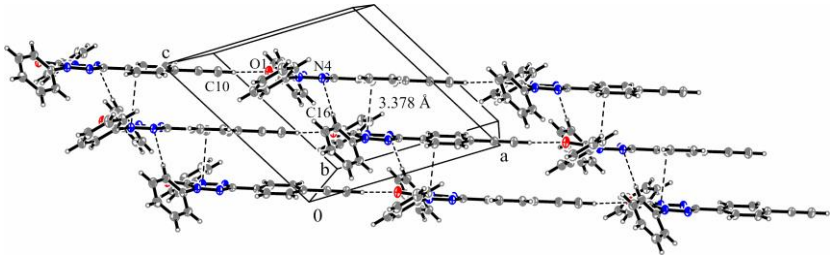


**Figure S7** Packing diagram presenting the formation of linear chains involving C-H···O interactions and their additional π ··· π and C-H···N interactions which are responsible for coupling $J_1$ in compound **5**

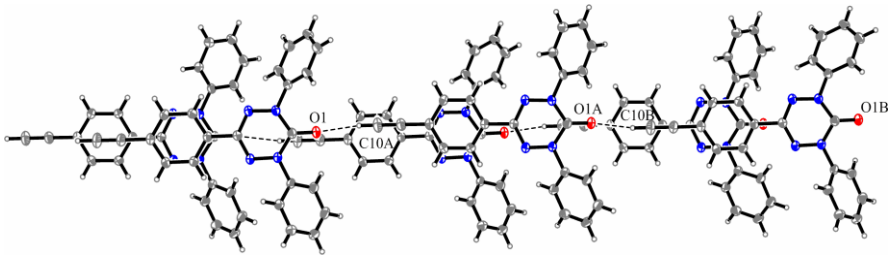


**Figure S8** View indicating the overlapping of the verdazyl-phenyl units in compound **5**

## Magnetic Measurements

The magnetic properties of verdazyl radical **1** were described before.[3] Details about the measurements for radicals **2**, **3**, **4** and **5** are given in the main article.

### Verdazyl Radical 2

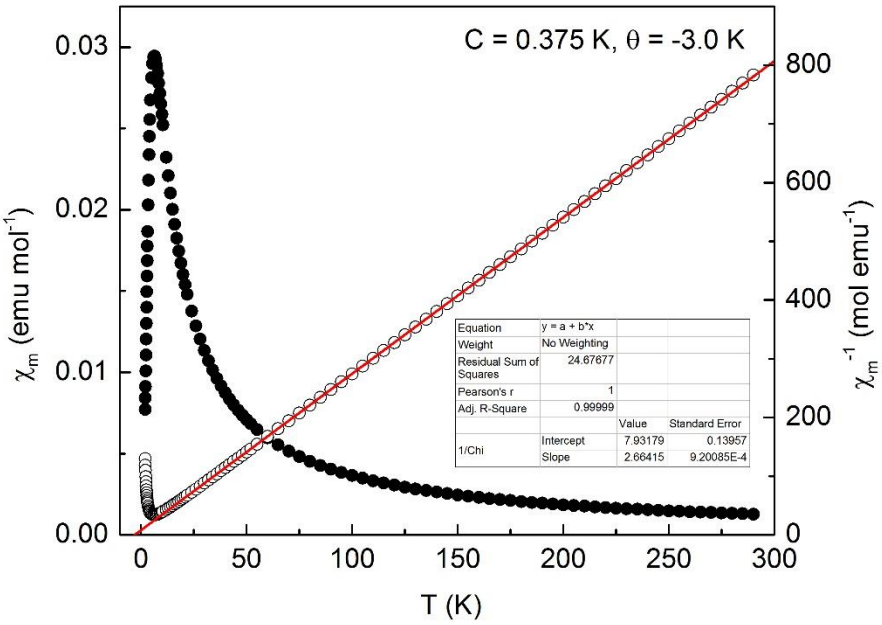


**Figure S9** Magnetic susceptibility vs. temperature plot for verdazyl radical **2**.

## Verdazyl Radical 3

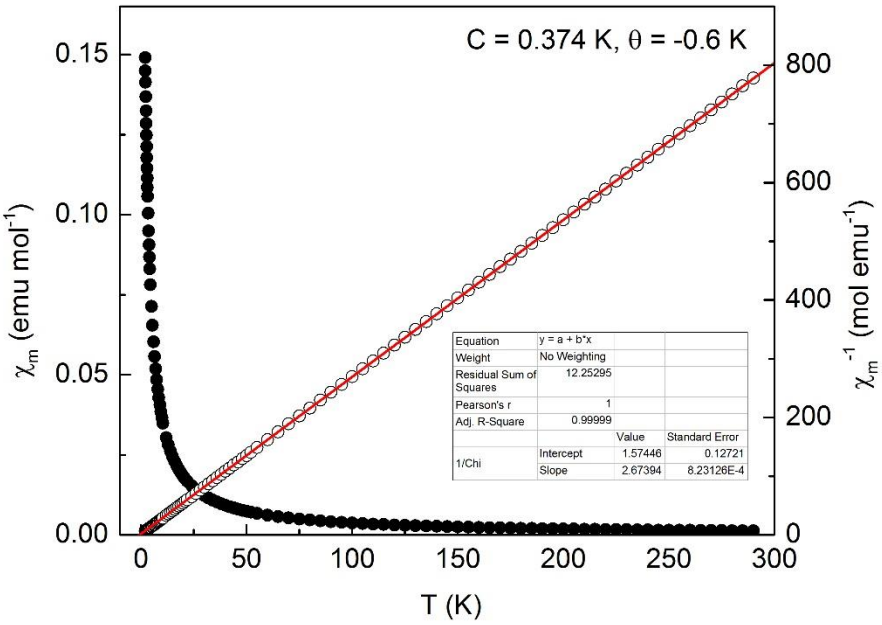


**Figure S10** Magnetic susceptibility vs. temperature plot for verdazyl radical **3**.

## Verdazyl Radical 4

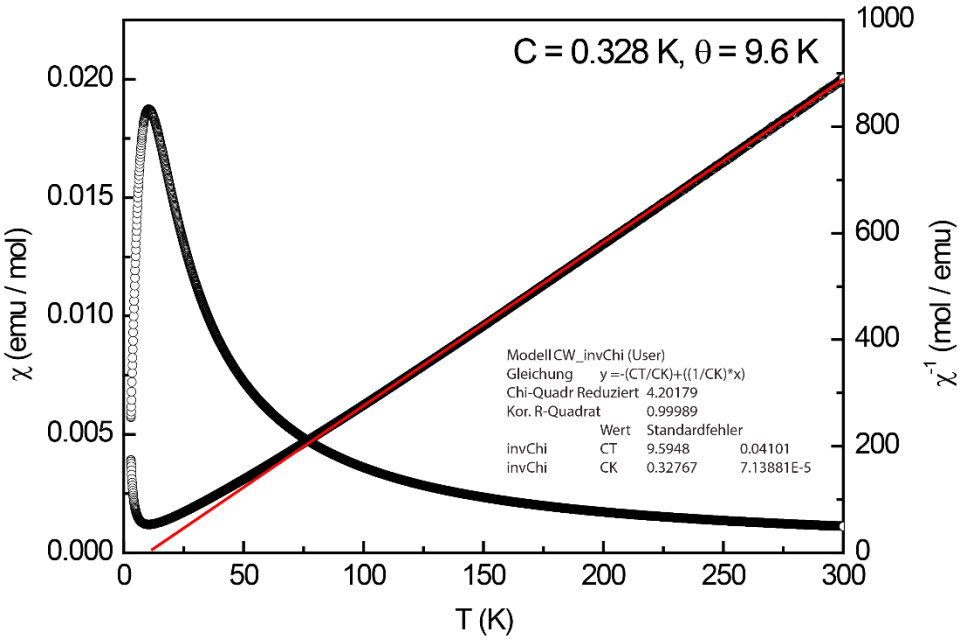


**Figure S11** Magnetic susceptibility vs. temperature plot for verdazyl radical **4**.

**Verdazyl Radical 5**

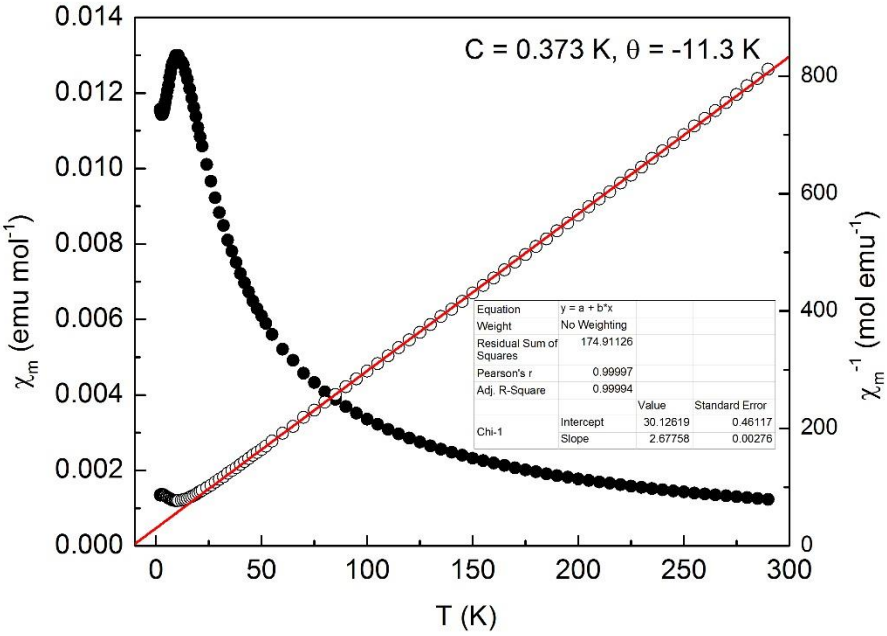


**Figure S12** Magnetic susceptibility vs. temperature plot for verdazyl radical **5**.

## $^{1}$H-NMR and $^{13}$C-NMR spectra for compound S1

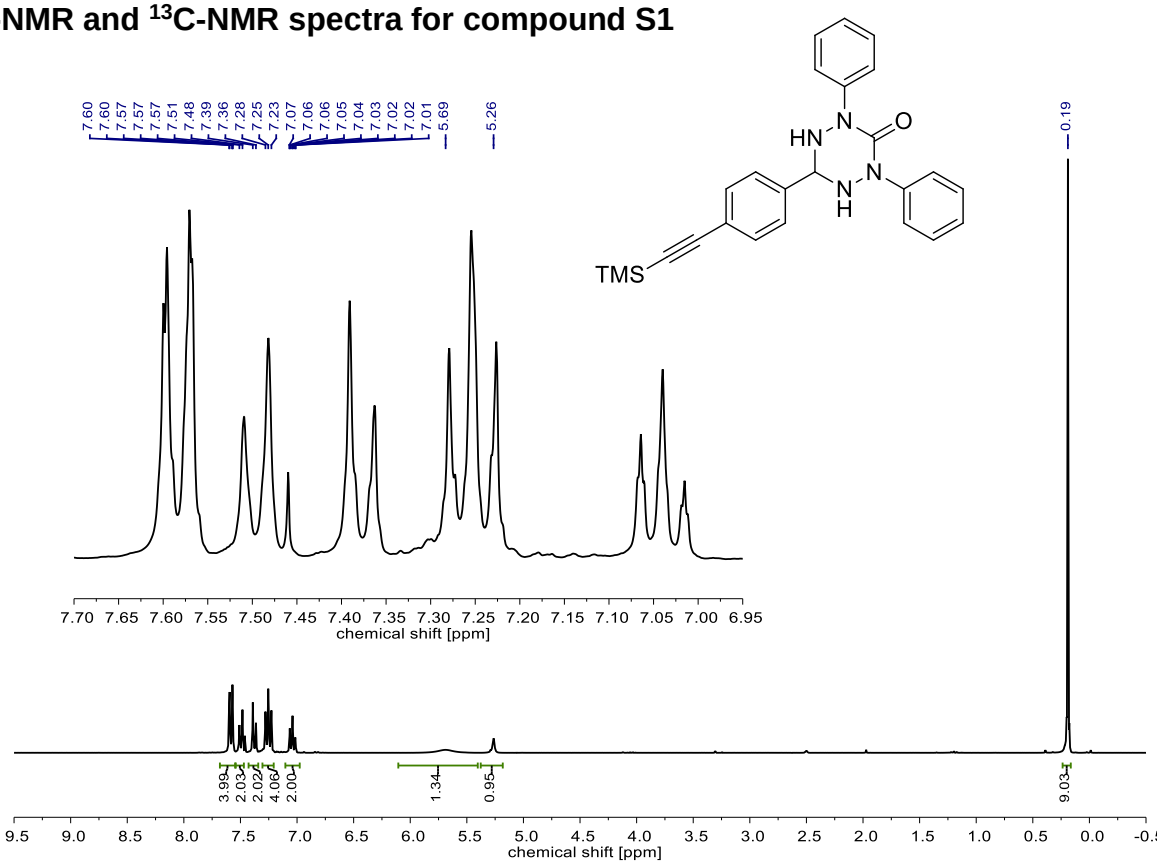


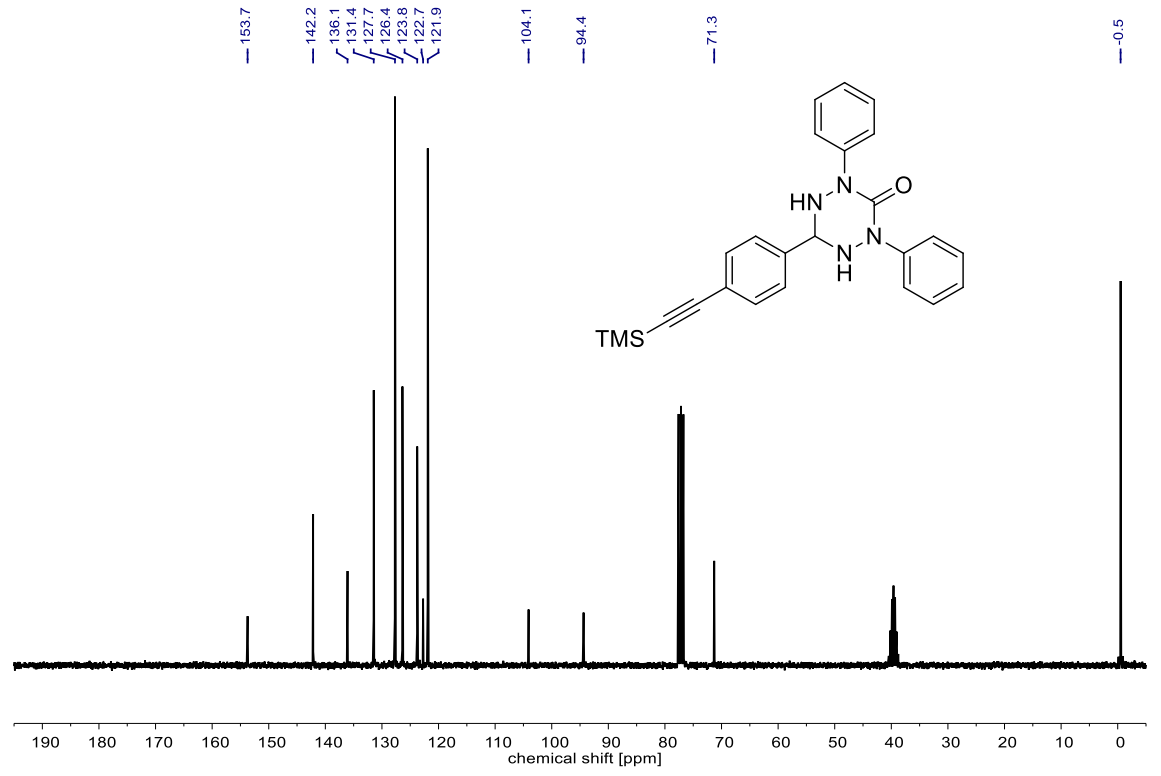

## Results for a Thiooxo-Verdazyl[4]

To additionally test our procedure, we applied it to another published verdazyl system[4]. The authors synthesized an adduct of 1,5-dimethyl-3-(2'-pyrid-yl)-6-thiooxoverdazyl radical (Svdpy) with hydroquinone (hq). Crystal structures are available for three different temperatures (100 K, 200 K and 303 K). We focus our discussion on the structure measured at the lowest temperature (100 K). The hq molecules, which rather have an influence on the structure than on the magnetic properties, were ignored during the procedure.

We found that those couplings, which were also discussed by the authors of the original work, are the strongest of the system with $J_1 = -3.46$ cm$^{-1}$ and $J_2 = -2.56$ cm$^{-1}$. Additionally, we found two ferromagnetic couplings with $J_3 = 0.89$ cm$^{-1}$ and $J_4 = 0.79$ cm$^{-1}$. As can be seen by comparing the red and green or the red and blue curves in Figure S13, the latter couplings have a visible but still small effect.

In agreement with the original authors we observe significant temperature effects (compare the red, purple and turquoise curves in Figure S13). However, we cannot observe a change in the sign of any coupling constant. Especially the results obtained for the lowest-temperature structure are in very good agreement with the experimental data shown in the original paper. The differences between our calculated data and the theoretical results in Ref. 4 can easily be explained through the different electronic-structure methods employed.

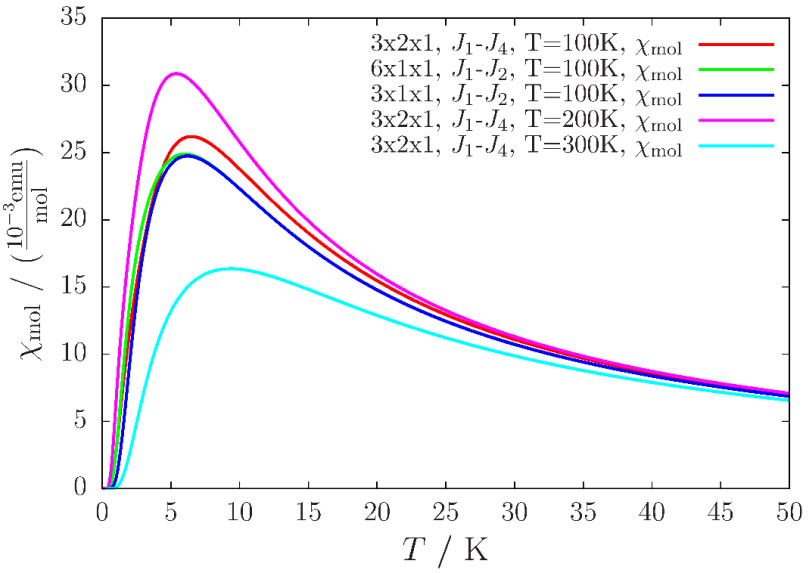


**Figure S13** Magnetic susceptibility vs. temperature plot for the thiooxo-verdazyl radical discussed in the text, calculated for magnetic models of different sizes and based on structures obtained at different temperatures.

## Further Details of the Computational Procedure

### Identification of Symmetries

Our procedure does not require any symmetry information as user input. Instead, the program itself checks for symmetry relations between the molecules and interactions. For these checks a symmetry operation is applied to a molecule and the result is compared to the other molecules by calculating the distances between corresponding pairs of atoms. A threshold of $10^{-4}$ Å was found to be suitable for atoms to be equal with respect to the finite accuracy of crystal structures.

Symmetry operations which are currently supported are: $C_2$ and $C_4$ rotations, mirror planes orthogonal to the cell vectors, inversion at the center of the cell and combinations of translations along the cell vectors with the mentioned symmetry operations. Additional symmetry operations may, however, easily be added to the existing ones through their matrix representations.

### Implementation Details About the Creation of a Magnetic Unit Cell

In order to find all periodic interaction chains we rely on a brute force strategy. Starting with the strongest coupling we form all possible chains of interactions by trying to attach the next coupling to all currently existing chains. If a chain can be extended, also the chain without the new coupling is kept in memory. Furthermore, we check whether two chains can be interlinked with the new coupling. The new coupling also defines an interaction chain on its own. Note that it is very well possible that the same coupling is part of many interaction chains.

After the introduction of a new coupling the list of interaction chains is filtered to erase rings, i.e. chains which end up at their own starting point, and identical chains. Whenever a chain becomes periodic (see Section 2.4.2. in the main article) it is not extended any more, but stored as a candidate for an axis of the magnetic unit cell.

Especially in systems with a small number of interactions between the magnetic sites different parts of the total system are sometimes not connected to each other through any coupling. In such a case the different subsystems can be treated independently from each other. Our program identifies and exploits such situations. As a consequence, the number of magnetic sites in a subsystem may be much smaller than in the whole system so that the setup and diagonalization of the Heisenberg Hamiltonian becomes significantly easier in terms of computational effort.

### Automated Choice of Magnetic Models Suitable for the Convergence Check

For an automated choice of magnetic models suitable for the convergence check discussed in Section 2.6 of the main article first, one model is picked as a reference model, which is assumed to be the best converged treatable model. Unfortunately, it cannot be easily predicted how quickly

the model converges into each of the directions. If convergence is not reached in this standard protocol other models can still be chosen as the reference. In the reference model all directions are considered approximately equally important. If the model with maximum size reached under this condition can still be extended into one or two more directions this is done with a priority on the first and then the second axis. For the three-dimensional case with $N_x$, $N_y$ and $N_z$ repititions of the magnetic unit cell along its three axes we thus obtain

$$N_z = \mathrm{int}\left[\left(\frac{N}{Z}\right)^{\frac{1}{3}}\right], \qquad N_y = \mathrm{int}\left[\left(\frac{N}{Z}/N_z\right)^{\frac{1}{2}}\right], \qquad N_x = \mathrm{int}\left[\frac{N}{Z}/\left(N_z * N_y\right)\right],$$

where $\frac{N}{Z}$ is the maximum number of unit cells leading to a maximum of $N$ magnetic sites in a model for a system with $Z$ magnetic sites per unit cell and $\mathrm{int}[x]$ is the largest integer number smaller or equal to $x$. Note that $N_x \geq N_y \geq N_z$, where an inequality is possible if some of the numbers are rounded down to reach an integer number.

This reference model is then compared to models where $N_\mu$ with $\mu \in \{x, y, z\}$ is reduced by one. If this is not possible, because $N_\mu$ already equals one, the program tries to find a different pair of models for the convergence check into that dimension. If this also fails a warning is issued so that it is left to the user to work out a strategy to test the convergence of that particular system.

**Choice of the Error Criterion**

The development of the magnetic susceptibility at high temperatures is dominated by Curie's law and will thus drop to zero irrespective of the actual magnetic properties of the system. Thus, in general an error criterion should ideally emphasize the low temperature region, where the actual properties of the system do have a large influence. For antiferromagnetic systems such a strategy could be successful. Unfortunately, the magnetic susceptibility of a ferromagnetic system raises to infinity for temperatures approaching 0 K. As a consequence, a tiny deviation in the magnetic properties of two systems or two different models of the same system can quickly lead to very large deviations at small temperatures. A further emphasis on this temperature region would thus not be suited to assess the quality of a model for a ferromagnetic system. Thus, we chose to not use a weighting scheme, but only calculate the mean average error to investigate the differences between two susceptibility curves as stated in Section 2.6 of the main article.

## References

(1) Masuda, Y.; Kuratsu, M.; Suzuki, S.; Kozaki, M.; Shiomi, D.; Sato, K.; Takui, T.; Okada, K. *Polyhedron* **2009**, *28*, 1950.

(2) Matuschek, D.; Eusterwiemann, S.; Stegemann, L.; Doerenkamp, C.; Wibbeling, B.; Daniliuc, C. G.; Doltsinis, N. L.; Strassert, C. A.; Eckert, H.; Studer, A. *Chem. Sci.* **2015**, *6*, 4712.

(3) Merhi, A.; Roisnel, T.; Rigaut, S.; Train, C.; Norel, L. *CrystEngComm* **2014**, *16*, 9783.

(4) Verot, M.; Brefuel, N.; Pecaut, J.; Train, C.; Robert, V. *Chem. Asian J.* **2012**, *7*, 380.